Highly Efficient Second-Harmonic Generation in Monolithic Matching Layer Enhanced $Al_xGa_{1-x}As$ Bragg Reflection Waveguides

Payam Abolghasem, *Student Member, IEEE*, Junbo Han, Bhavin J. Bijlani, *Student Member, IEEE*, Arghavan Arjmand, *Student Member, IEEE*, and Amr S. Helmy, *Senior Member, IEEE*

***Abstract*—In this letter, we demonstrate significant improvement in second-harmonic (SH) generation using matching layer enhanced $Al_xGa_{1-x}As$ Bragg reflection waveguide in type-I and type-II phase-matching schemes. For a 1.8-ps pulsed pump around 1550 nm with an average power of 3.3 mW, peak SH powers of 28 and 60 μW were measured in type-I and type-II interactions, respectively. The associated normalized conversion efficiencies were estimated to be $5.30 \times 10^3\,\%$ and $1.14 \times 10^4\,\%\ W^{-1} \cdot cm^{-2}$ with SH process bandwidths of 1.7- and 1.8-nm full-width at half-maximum. Waveguides with various ridge widths ranging between 2.8 and 4.8 μm with 2.17-mm length were characterized.**

***Index Terms*—Bragg reflection waveguides (BRWs), nonlinear optics, optical nonlinearities in semiconductors, phase matching, second-harmonic generation (SHG), second-order nonlinearities.**

I. Introduction

THE LACK of an efficient second-order nonlinear phase-matching (PM) technique in $Al_xGa_{1-x}As$ is a major hindrance to advanced integrated devices. A suitable integration platform that incorporates active and nonlinear elements has so far eluded researchers. Without it, compact parametric devices such as integrated optical parametric oscillators (OPOs) and integrated photon-pair sources cannot be realized. To date, several PM schemes, such as form birefringence [1], domain-reversal quasi-PM [2], and modal PM [3], have been investigated. Among these, form birefringence has received the greatest attention as an efficient PM technique. The existence of oxide layers in form birefringence, an essential component for attaining artificial birefringence, makes it virtually impossible to monolithically incorporate active components such as electrically driven laser diodes.

Recently, we have demonstrated a PM scheme using Bragg reflection waveguides (BRWs) [4], [5], which offers a robust platform for monolithic integration of diode laser pump with nonlinear frequency conversion element. Phase-matching using BRWs is an exact PM technique, which employs strong modal dispersion properties of propagating modes in a photonic bandgap device. Unlike conventional modal phase-matching schemes [3] where PM is attained between higher order modes, BRWs offer PM between the lowest order modes of the involved frequencies. This allows maximum utilization of the pump power for the nonlinear interaction. So far, theoretical and experimental endeavors have been widely focused on utilizing quarter-wave BRWs (QtW-BRWs), where the bilayers of transverse Bragg reflectors (TBRs) are quarter-wave thick. Operating at the quarter-wave condition is attractive due to simple design equations, polarization degeneracy of the fundamental mode, and versatile dispersion properties [4]. However, the quarter-wave condition imposes constraints over the waveguide design that limits the efficiency of these devices in nonlinear frequency conversion. For example, phase-matched QtW-BRWs have small core dimensions, resulting in poor confinement factor and degraded nonlinear interaction.

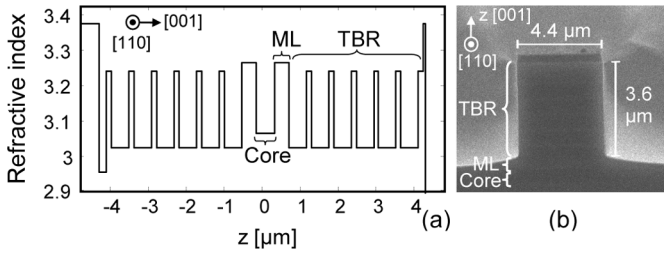

Fig. 1. (a) Index profile of ML enhanced BRW at pump wavelength. (b) Cross section SEM of a characterized waveguide.

Here, we discuss the first demonstration of a modified BRW that utilizes an additional layer, referred to as matching layer (ML), located between the core and the Bragg mirrors [6] [see Fig. 1(a)]. In the proposed structure, the constraint over the core thickness is relaxed while the thickness of the ML is designed, such that the propagating Bragg mode experiences an electric or magnetic node at the interface between the ML and the periodic claddings. In this sense, the bilayers of the TBRs remain quarter-wave thick, allowing one to benefit from quarter-wave stacks, while the inclusion of the ML provides high flexibility in tailoring dispersion properties, linear, and nonlinear properties [7]. The experimental results discussed here illustrates a new record-high nonlinear conversion efficiency for this class of waveguides.

Manuscript received May 04, 2009; revised June 24, 2009. First published July 24, 2009; current version published September 18, 2009. This work was supported in part by the Natural Sciences and Engineering Research Council of Canada, in part by the Ontario Centres of Excellence, and in part by CMC Microsystems.

The authors are with The Edward S. Rogers Sr. Department of Electrical and Computer Engineering and the Institute of Optical Sciences, University of Toronto, Toronto, ON M5S 3G4, Canada (e-mail: payam.abolghasem@utoronto.ca; junbo.han@utoronto.ca; b.bijlani@utoronto.ca; arghavan.arjmand@utoronto.ca; a.helmy@utoronto.ca).

Color versions of one or more of the figures in this letter are available online at http://ieeexplore.ieee.org.

Digital Object Identifier 10.1109/LPT.2009.2027996

II. Device Structure and Fabrication

The wafer was grown on a nominally undoped GaAs [100] substrate using metal–organic chemical vapor deposition (MOCVD). It had a 200-nm $Al_{0.85}Ga_{0.15}As$ buffer grown on the substrate. The core was $Al_{0.61}Ga_{0.39}As$ with 500-nm thickness. The ML was 375-nm-thick $Al_{0.20}Ga_{0.80}As$. The TBRs were symmetric with respect to the core and consisted of six periods of $Al_{0.70}Ga_{0.30}As$–$Al_{0.25}Ga_{0.75}As$ with associated thicknesses of 129 nm/461 nm. The wafer was capped by a 50-nm GaAs. Ridge waveguides with variable widths ranging between 2.8 and 4.8 μm were patterned along [110] direction by dry etching the wafer to a depth of 3.6 μm. The waveguides had a length of 2.17 mm. An SEM micrograph of a characterized waveguide is shown in Fig. 1(b).

III. Characterization Results

The waveguide's linear properties were characterized using Fabry–Pérot method with a single-mode tunable laser source in the wavelength range of 1550–1560 nm. Best device performance was obtained for a waveguide with a ridge size of 4.4 μm. For this waveguide, loss values for TE and hybrid TE+TM [electric field at 45° with respect to the z axis in Fig. 1(b)] polarization states were measured as 2.0 and 2.2 cm^{-1}, respectively. Fresnel reflection at the waveguide facets were estimated to be 29%. Linear coupling efficiency due to spatial overlap between the pump beam and the excited fundamental mode was measured to be 49%. It is worth mentioning that the estimation of linear characteristics of BRWs can be problematic as a result of the support for multimode propagation. However, the clear Fabry–Pèrot fringes of the transmitted spectrum ensured the detection of only the lowest order mode of the pump (FH) as desired. Although, higher order modes were likely excited at the front facet, they were filtered out from the transmitted spectrum through loss discrimination mechanism.

Characterization of waveguide nonlinear properties was carried out in an end-fire rig setup using a mode-locked Ti : sapphire pumped OPO. The employed pulses had a temporal width of 1.8 ps with a repetition rate of 76 MHz. The pulses were nearly transform limited with a temporal-spectral bandwidth product of $\Delta\tau\Delta\nu = 0.53$. A 40× diode objective lens was used at the input stage for coupling light into the waveguide. The emerging signal was collected using a 40× objective lens. A long wavelength pass filter was used in the output stage to separate the pump from the second harmonic. We examined both type-I and type-II nonlinear interactions. To investigate the polarization state of the frequency doubled signal, a polarization beam splitter was used before a silicon detector. Initially, we obtained the second-harmonic generation (SHG) tuning curve by monitoring second-harmonic (SH) power as a function of the pump wavelength for a fixed pump power of 9.6 mW, measured before the input objective lens. Accounting for the transmission of the input objective lens (98%), facet reflection, and end-fire coupling factor, the internal pump power P_{FH} estimated after the waveguide front facet was obtained to be 3.3 mW. For type-I and type-II interactions, peak SH power of 16 and 33 μW, respectively, was measured at the detector. Taking into consideration the transmission of the output objective lens (81%), reflection of long wavelength pass filter (96%), and the facet reflection, we estimate internal SH powers to be 28 and 60 μW for type-I and type-II PMs, respectively. The resulting tuning curves are shown in Fig. 2, where the associated PM wavelengths were detected at 1551 and 1555 nm. Also, in Fig. 2 (inset), we have plotted the SH power versus pump power on a log–log scale at PM wavelengths. The approximate slope values of two correspond well to the quadratic dependence between the powers of SH and that of the pump in an ideal lossless process. The deviation of the harmonics power relation from a perfect quadratic relation is accounted for by multiphoton absorption, particularly at high pump power.

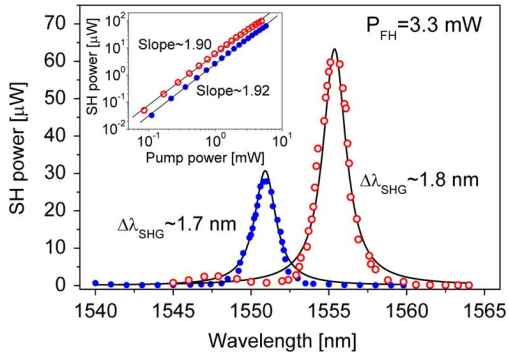

Fig. 2. Measured SH power as a function of pump wavelength in type-I (filled circle) and type-II (circle) interactions for a fixed internal pump power of $P_{\mathrm{FH}} = 3.3$ mW. The solid lines are the best fits to Lorentzian function. (Inset) Dependency of SH power on that of the pump plotted on a log–log scale.

A figure of merit that indicates the waveguide performance in SHG is the normalized internal conversion efficiency defined as $\eta = P_{\mathrm{SH}}/(P_{\mathrm{FH}}^2 L^2)$, where P_{SH} is the internal SH power and L is the waveguide length. As such, we derive the efficiencies for type-I and type-II PMs as $5.30 \times 10^3\%$ and $1.14 \times 10^4\%$ $W^{-1} \cdot cm^{-2}$, respectively. In comparison to a previous design with QtW-BRW [5], the estimated values of η here denote an enhancement by over an order of magnitude, which highlights the improvement offered by the ML structure. Also, it would be informative to compare the efficiency of our device with the work in [1], where, to the best of our knowledge, record-high SHG conversion was measured in a type-I birefringently phase-matched (BPM) GaAs–Al_2O_3 waveguide. In the referenced work, 200-fs pulses were used in a 1-mm-long waveguide. SH power of 650 μW was then detected for a pump with 5 mW internal power. We extract the pulse conversion efficiency of [1] to be $2.6 \times 10^5\%$ $W^{-1} \cdot cm^{-2}$. Our type-I and type-II interactions are less efficient by approximately 1.7 and 1.4 orders of magnitude, respectively, when compared with the BPM sample. However, a more meaningful comparison can be obtained by mapping the value of η in [1] into the picosecond regime. Such conversion is derived by calculating the ratio of the pulse duty cycles in [1] (1.8×10^{-5}) to that in our experiment (1.37×10^{-4}). As such, the femtosecond conversion efficiency in [1] is scaled down with a calculated factor of 0.13 to an "equivalent" picosecond value of $3.38 \times 10^4\%$ $W^{-1} \cdot cm^{-2}$. This compensated value is within the same order of magnitude as our measured type II interaction. We further stress that the actual conversion efficiencies of our structure were indeed larger

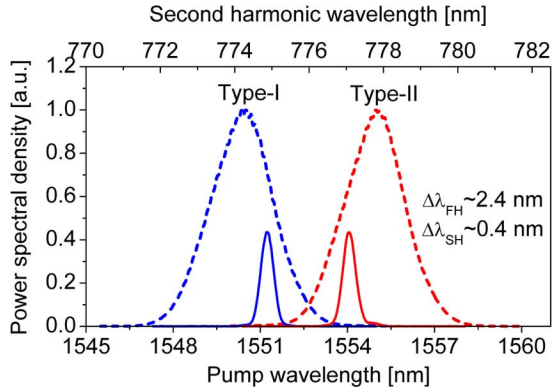

Fig. 3. Spectra of the pump (dashed line) with an FWHM bandwidth of $\approx$2.4 nm and the corresponding SH spectra (solid line) in type-I and type-II interactions.

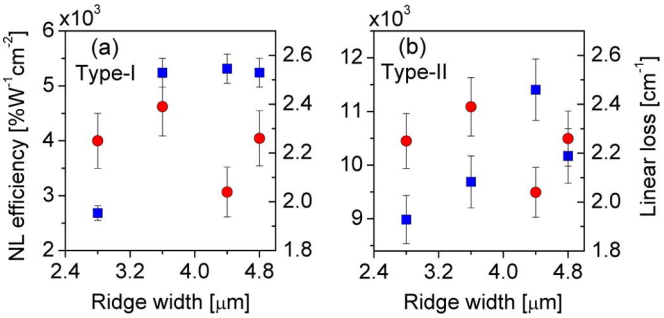

Fig. 4. Normalized conversion efficiency (squares) and linear propagation loss (circles) as a function of waveguide ridge width for: (a) type-I and (b) type-II PM.

than our calculated values here. This claim is supported by the fact that in our calculations of η, the collection efficiency of the output objective lens was considered to be 100%. Due to the fast divergence of BRW modes from the output facet, only a part of the generated SH power is collected during the experiment.

The power spectral densities of the harmonics at the PM wavelengths are illustrated in Fig. 3. From the figure, the full-width at half-maximum (FWHM) bandwidths of the pump (dashed line) and SH (solid line) were measured to be 2.4 and 0.4 nm, respectively. The narrower SH spectrum clearly indicates that only a portion of the pump spectrum was utilized during the nonlinear interaction. Further improvements in nonlinear conversion can be expected by incorporating a pump signal with closer spectrum match with that of SH.

We further characterized linear/nonlinear properties of waveguides with ridge sizes 2.8, 3.6, and 4.8 μm. Of particular interest was to investigate any correlation between linear propagation loss (α) and nonlinear conversion efficiency (η). In Fig. 4, we have plotted α and η as functions of the ridge size for both type-I and type-II PMs. In the figure, a clear correlation between α and η cannot be established for either nonlinear interactions. For example, consider type-I process in waveguides with 2.8 and 4.8 μm ridge widths. Although in this case, the linear loss of both waveguides were approximately the same (2.3 cm^{-1}), the conversion efficiency of the former was almost half of that of the latter waveguide. This behavior indicates that the nonlinear conversion efficiency is not sensitive to observed variations of the fundamental propagation loss. Rather, we speculate that the SH loss plays a more significant role on the nonlinear conversion efficiency. Due to the leaky nature of the Bragg mode, direct measurement of SH loss is extremely challenging in these structures. However, we obtained a rough estimation of SH loss by fitting experimental tuning curves to a Lorentzian function where the FWHM bandwidth of the fit was associated with the loss value [8]. For the waveguide with 4.4 μm ridge size, SH loss values of 43 and 46 cm^{-1} were obtained for type I and type II, respectively.

IV. Conclusion

In summary, first, demonstration of efficient phase-matching of SHG using BRW-MLs was presented. The nonlinear conversion efficiency in type-II interaction was in proximity to the record-high conversion measured in birefringence phase-matched GaAs–Al_2O_3 waveguides. BRW-MLs, however, benefit from being more amenable to monolithic integration with active components, with ample room for optimization through reducing propagation losses, improving nonlinear overlap factor, and minimizing the group velocity mismatch to enable longer interaction lengths.

Acknowledgment

The authors would like to acknowledge the support of J. S. Aitchison for the pulsed characterization setup

References

[1] K. Moutzouris, S. V. Rao, M. Ebrahimzadeh, A. De Rossi, V. Berger, M. Calligaro, and V. Ortiz, "Efficient second-harmonic generation in birefringently phase-matched GaAs/Al_2O_3 waveguides," *Opt. Lett.*, vol. 26, no. 22, pp. 1785–1787, Nov. 2001.

[2] X. Yu, L. Scaccabarozzi, J. S. Harris, P. S. Kuo, and M. M. Fejer, "Efficient continuous wave second harmonic generation pumped at 1.55 μm in quasi-phase-matched AlGaAs waveguides," *Opt. Express*, vol. 13, no. 26, pp. 10742–10748, Dec. 2005.

[3] K. Moutzouris, S. V. Rao, M. Ebrahimzadeh, A. De Rossi, M. Calligaro, V. Ortiz, and V. Berger, "Second-harmonic generation through optimized modal phase matching in semiconductor waveguides," *Appl. Phys. Lett.*, vol. 83, no. 4, pp. 620–622, Jul. 2003.

[4] B. R. West and A. S. Helmy, "Analysis and design equations for phase matching using Bragg reflection waveguides," *IEEE J. Sel. Topics Quantum Electron.*, vol. 12, no. 3, pp. 431–442, May/Jun. 2006.

[5] B. Bijlani, P. Abolghasem, and A. S. Helmy, "Second harmonic generation in ridge Bragg reflection waveguides," *Appl. Phys. Lett.*, vol. 92, no. 10, pp. 101124-1–101124-3, Mar. 2008.

[6] A. Mizrahi and L. Schächter, "Bragg reflection waveguides with a matching layer," *Opt. Express*, vol. 12, no. 14, pp. 3156–3170, Jul. 2004.

[7] P. Abolghasem and A. S. Helmy, "Matching layers in Bragg reflection waveguides for enhanced nonlinear interaction," *IEEE J. Quantum Electron.*, vol. 45, no. 6, pp. 646–653, Jun. 2009.

[8] A. Fiore, S. Janz, L. Delobel, P. van der Meer, P. Bravetti, V. Berger, E. Rosencher, and J. Nagle, "Second-harmonic generation at $\lambda = 1.6\,\mu$m in AlGaAs/Al_2O_3 waveguides using birefringence phase matching," *Appl. Phys. Lett.*, vol. 72, no. 23, pp. 2942–2944, Jun. 1998.